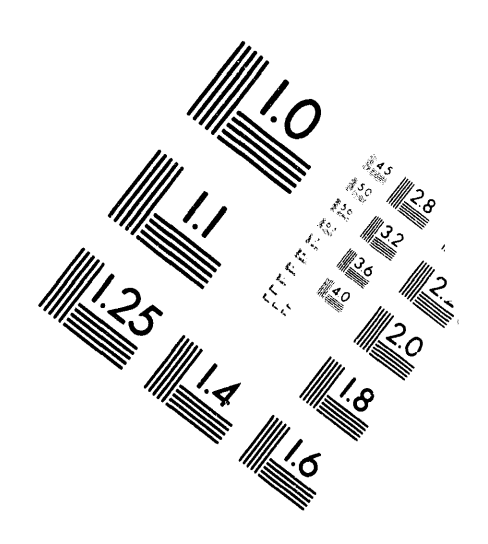
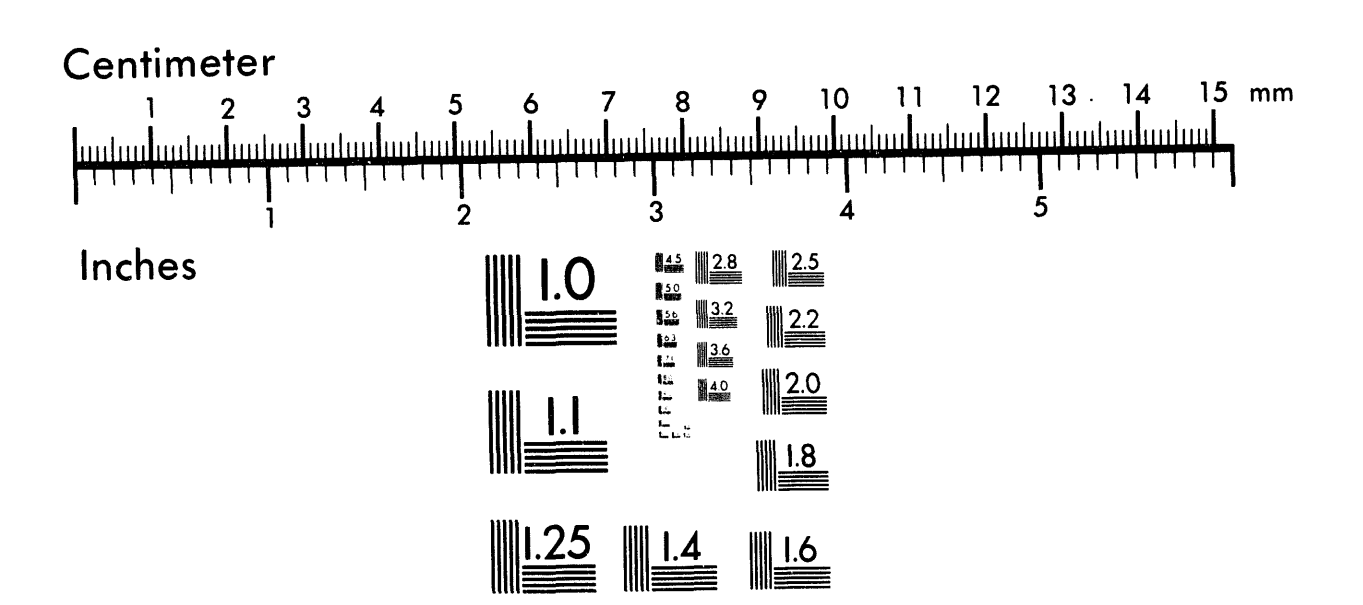


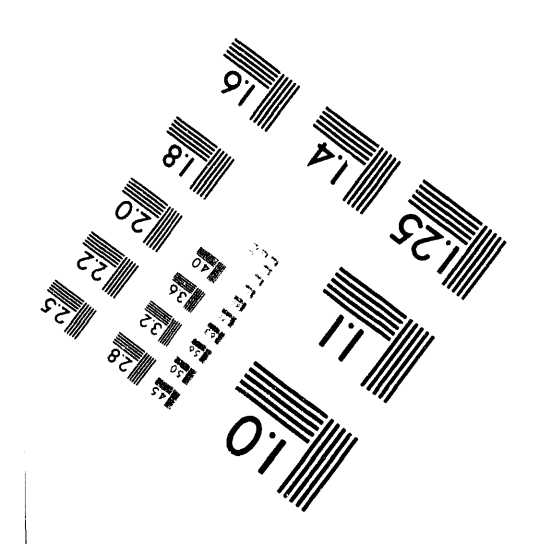


Association for Information and Image Management

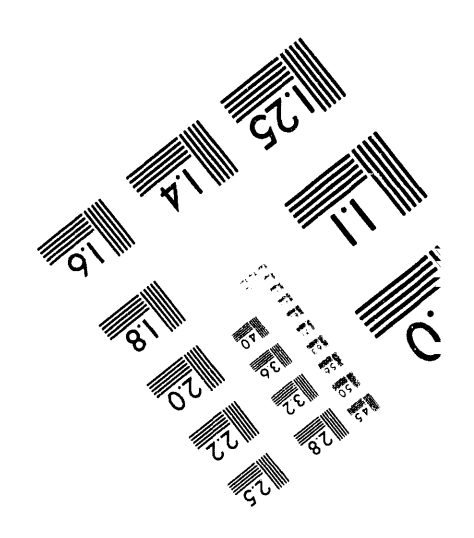
1100 Wayne Avenue, Suite 1100 Silver Spring, Maryland 20910 301/587-8202







MANUFACTURED TO AIIM STANDARDS
BY APPLIED IMAGE, J.NC.



2

Conf-9306210--2

Cavity-QED Enhancement of Fluorescence Yields in Microdroplets

Michael D. Barnes, William B. Whitten, and J. Michael Ramsey

Analytical Chemistry Division Oak Ridge National Laboratory Mail Stop 6142 Oak Ridge, Tennessee 37831

"The submitted menuscript has been authored by a contractor of the U.S. Government under contract No. DE-AC05-840R21400. Accordingly, the U.S. Government retains a nonexclusive, royalty-free license to publish or reproduce the published form of this contribution, or allow others to do so, for U.S. Government

RECENT SUBMITTED PUBLICATIONS

- (1) M. D. Barnes, W. B. Whitten, and J. M. Ramsey, "Enhanced Fluorescence Yields Through Cavity-QED Effects in Microdroplets," J. Opt. Soc. Am. B. submitted, July, 1993.
- (2) M. D. Barnes, K. C. Ng, W. B. Whitten, and J. M. Ramsey, "Detection of Single Rhodamine 6G Molecules in Levitated Microdroplets," Anal. Chem. 65, 2360 (1993).
- (3) M. D. Barnes, W. B. Whitten, S. Arnold, and J. M. Ramsey, "Homogeneous Linewidths of Rhodamine 6G at Room Temperature from Cavity-Enhanced Spontaneous Emission Rates," J. Chem. Phys. 97, 7842 (1992).

Abstract

Measurements of the integrated fluorescence yield of Rhodamine 6G (R6G) in levitated microdroplets (4 to 16 μ m diameter) display a size dependence which is attributed to a decreased probability per excitation cycle of photochemical bleaching as a result of cavity-enhanced spontaneous emission rates. The average number of fluorescence photons detected per molecule in 4 μ m droplets (where emission rate enhancement has been previously demonstrated) is shown to be approximately a factor of 2 larger than the yield measured for larger droplets where emission rate enhancement does not occur. Within some simple approximations, these results suggest that essentially no emission rate inhibition occurs in this system. A mechanism based on spectral diffusion is postulated for the apparent absence of cavity-inhibited emission and is illustrated by Monte Carlo calculations using time-dependent lineshape functions.

Research sponsored by U.S. Department of Energy, Office of Basic Energy Sciences, under Contract DE-AC05-840R21400 with Martin Marietta Energy Systems, Inc.'



Introduction

One of the fundamental sensitivity limitations in the fluorescence detection of single dye molecules in solution is the finite number of photons which can be emitted by the molecule before irreversible photochemical bleaching occurs, or fluorescence vield. The fluorescence yield is directly proportional to the spontaneous emission rate,²,³ however, in bulk solution, the emission rate of a particular molecule is essentially fixed for a given solvent. It is now well-known that the spontaneous emission rate of atoms or molecules can be modified (enhanced or inhibited) by placing the emitting species in a small-volume optical enclosure.4,5 Recently, it has been shown that the spontaneous emission rate can be significantly enhanced in a microdroplet environment for dye molecules and chelated ions through coupling of emission into morphology dependent resonances (MDRs) of the droplet. This effect could, in principle, increase the fluorescence yield for dye molecules thereby increasing sensitivity. However, since the emission profile overlaps several droplet MDRs, cavity-inhibited emission^{8,9,10,11} was also initially expected to occur; thus it was unclear whether the combination of emission rate enhancement and inhibition would result in a net increase in the fluorescence yield.

Here we show that a significant increase in the fluorescence yield for R6G in 4 and 5 µm diameter glycerol microdroplets relative to the photon yield for larger droplets (> 10 µm diameter). These results indicate that the combined effects of emission rate enhancement and inhibition do not cancel completely. Using the previously measured emission rate constants, 6 the relative fraction of molecules whose emission rate is inhibited is estimated to be very nearly zero. We propose a model based on spectral diffusion 12 in which the transition frequency is not fixed but undergoes random shifts 13 as it is perturbed by the motion of the solvent in response to the change in the dipole moment of the chromophore upon excitation. On roughly the same time-scale as the (free-space) radiative lifetime, the width of a spectral line becomes dynamically broadened which allows the excited state to sample a progressively larger range of frequencies which eventually encompasses at least one droplet MDR.

Fermi's golden rule, ¹⁴ given in Eq. (1), provides a basic understanding of how emission rates may be modified in small-volume

optical cavities. The rate of spontaneous emission from state j to state i can be estimated from the expression

$$\mathbf{A}_{i \to j} = \frac{2\pi}{\hbar^2} \left\langle i \mid \mathbf{H}_{ij} \mid j \right\rangle^2 \rho(\omega) \tag{1}$$

where < i | Hij | j > is the (volume-normalized) Hamiltonian matrix element representing the atom-field interaction, and $\rho(\omega)$ is the density of final photon states at the emission frequency ω . In bulk media, $\rho(\omega)$ is essentially a constant over a small range of optical frequencies so the emission rate will be approximately independent of ω . When the dimensions of the optical enclosure become comparable to the emission wavelength, the vacuum photon state density becomes redistributed so that $\rho(\omega)$ is much larger than the free-space value when ω corresponds to a cavity resonance. Conversely, $\rho(\omega)$ is much smaller than the free-space value when ω is non-resonant. Therefore, the emission rate may be enhanced or inhibited depending on whether the emission frequency corresponds with a cavity resonance provided the cavity resonance spacing is much larger than the spectral linewidth. 16

For optical transitions, this condition implies cavity dimensions on the order of microns which can be satisfied by using micron-sized high-refractive index liquid droplets. Cavity effects in microdroplets are well known and arise from morphology dependent resonances (MDRs)¹⁷ of the droplet which occur at specific values of the size-parameter, X, defined as $X=2\pi r/\lambda$, where r is the radius of the sphere and λ is the wavelength of light. These resonances have very high Q's (10 3 - 10 8) and processes such as stimulated emission 18 and lasing $^{19},^{20}$ as well as enhanced energy transfer 21 have been reported in droplets. Recently, Campillo and co-workers 7 have reported enhancement (and inhibition) of the spontaneous emission rate for chelated europium ions in a stream of falling (10 μm diam.) ethanol droplets and demonstrated the unique frequency dependence of the enhanced emission.

In our previous investigation of the temporal distribution of fluorescence emission from R6G in levitated microdroplets,6 the fluorescence decay kinetics observed for larger droplets (\geq 10 μ m diam.) were found to be essentially the same as

in bulk solution. For smaller droplets (4 - 8 μ m diam.) however, the fluorescence decay showed two distinct decay components: a slow component with essentially the same time constant as the bulk, and a second much faster decay component whose relative amplitude and decay constant increased with decreasing droplet size. The increase in the decay constant of the fast component with decreasing droplet size was consistent with the expectation that the enhancement should be proportional to the free spectral range. ¹⁴ Analysis of these results showed that a 12-fold increase in the spontaneous emission rate constant occurs for R6G in 4 μ m diameter glycerol droplets over the decay constant measured in bulk solution.

Because the emission profile overlaps several droplet resonances, it was initially expected that an inhibited rate component should also occur due to emission at frequencies between the cavity resonances. However no inhibited emission was observed, and it was originally assumed that the absence of an inhibited rate component was due to experimental parameters in the time-correlated photon counting apparatus which emphasized the short-time behavior of the fluorescence emission. We have further investigated the question of cavity-inhibited emission of dye molecules in liquid microdroplets by examining the integrated fluorescence yield as a function of droplet size. Since the number of fluorescence photons emitted per molecule should be proportional to the rate constant for spontaneous emission averaged over all molecules in the droplet, the fluorescence yield should be sensitive to the relative fraction of molecules with enhanced and inhibited emission rates as well as the magnitude of emission rate enhancement and inhibition. For droplet diameters between 7 and 16 µm, the average fluorescence yield was observed to be independent of droplet size, while approximately a two-fold increase in the fluorescence yield was measured for 4 µm diameter droplets relative to the larger sizes. These results suggest that the combined effects of enhanced and inhibited emission rates do not cancel completely and further suggest that the fraction of molecules with an inhibited emission rate is very small.

Experimental

The experimental apparatus is similar to that previously described except that a second photomultiplier has been added to increase sensitivity. Briefly, a three-electrode structure similar to that employed in ion-trap mass spectrometers is used

to levitate glycerol droplets.²² Two f/1 collection optics view the droplet at +/- 135° with respect to the direction of propagation of the (cw) Ar+ excitation laser. The laser was horizontally polarized, with an intensity at the droplet of about 500 W/cm². A nominal total measurement time of 200 seconds was used to accurately determine the mean background level. R6G concentrations in glycerol ranged from 1 to 4 x 10-9 M, corresponding to about 100 molecules in the smallest droplets and a few thousand molecules in the largest ones.

Droplets were produced from a piezoelectric pipet²³ with a 40 μ m diameter orifice. Control over the droplet diameter was obtained by diluting the R6G/glycerol solutions with varying amounts of water. Droplets leave the pipet with approximately the same diameter as that of the pipet orifice and, after rapid evaporation of the water, a glycerol droplet is left whose volume is roughly proportional to the degree of dilution. Droplet diameters were determined with an estimated uncertainty of ≈ 10 % by measuring the distance between reflected and refracted glare-spots²⁴ from laser illumination using an eyepiece reticle with rulings corresponding to 1 μ m. At the end of a fluorescence measurement, the mean background is subtracted from the data set and the integrated fluorescence signal is normalized by dividing by the number of molecules in the droplet calculated from the concentration and droplet diameter. This normalized signal represents the average number of fluorescence photons emitted per molecule which we term the fluorescence yield.

Results and Discussion

Figure 1 shows the fluorescence count rate at both detectors versus time for a 10 μm glycerol droplet containing ≈ 1000 R6G molecules. The total number of fluorescence photons after background subtraction for this droplet was 5.5 x 106, giving a fluorescence yield of 5500 photons/molecule. Figure 2 shows the average fluorescence yield as a function of droplet diameter. About 10 droplets of a given size were analyzed and the error bars represent +/- 1 σ . For droplet diameters between 7 and 20 μm , the average fluorescence yield is 4800 photons/molecule and is independent of diameter. At droplet diameters of 5 and 4 μm , average fluorescence yields were determined to be 8900 and 10500 photons per molecule, respectively. Even though the relative uncertainty for the smaller droplets is larger due to the higher relative error in the diameter measurement, the increase in the average fluorescence yield of about a factor of 2 is clearly significant.

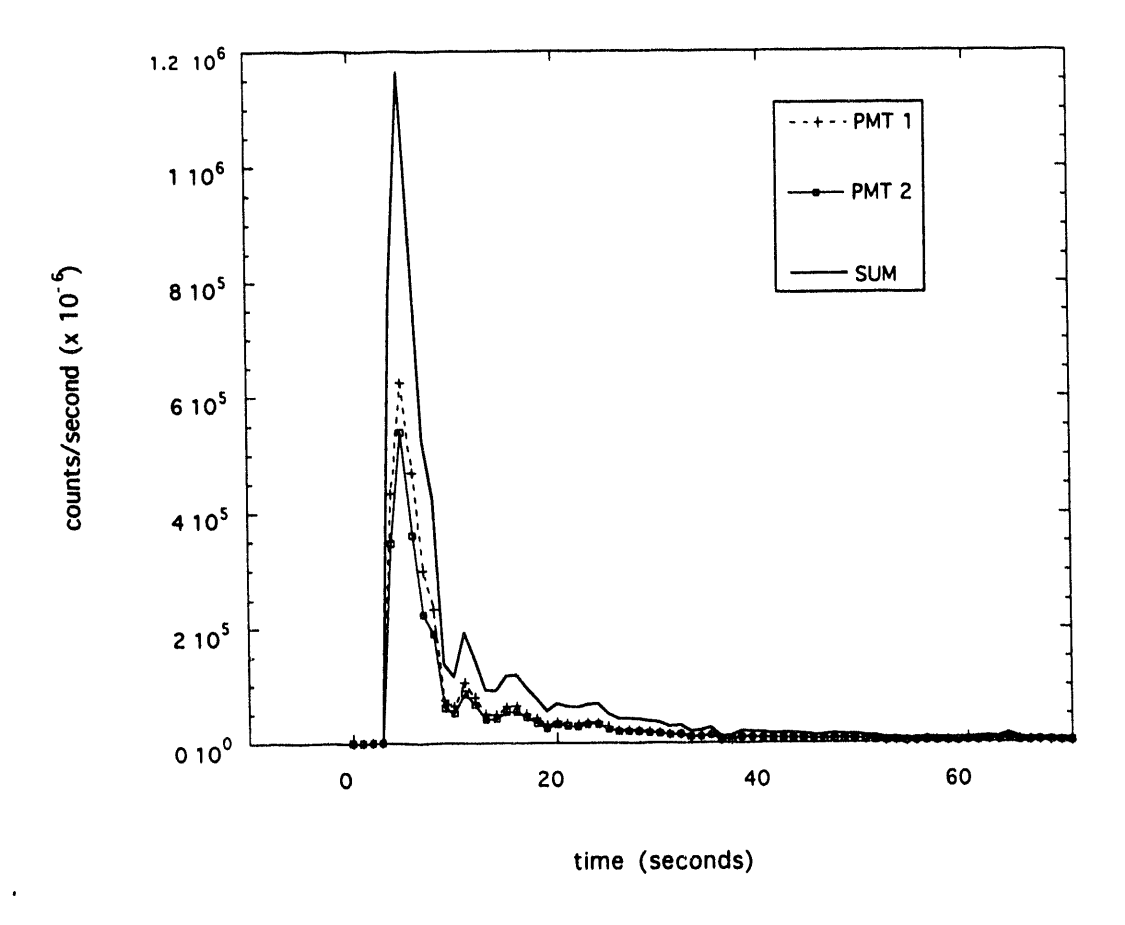


Figure 1. Typical two-channel fluorescence data for R6G (concentration was 3.16 x 10-9 M) in a 10 μ m glycerol droplet. The integrated signal is 5.5 x 106 counts. Dividing by the number of molecules in the droplet(\approx 1000) gives a fluorescence yield of 5500 photons/molecule.

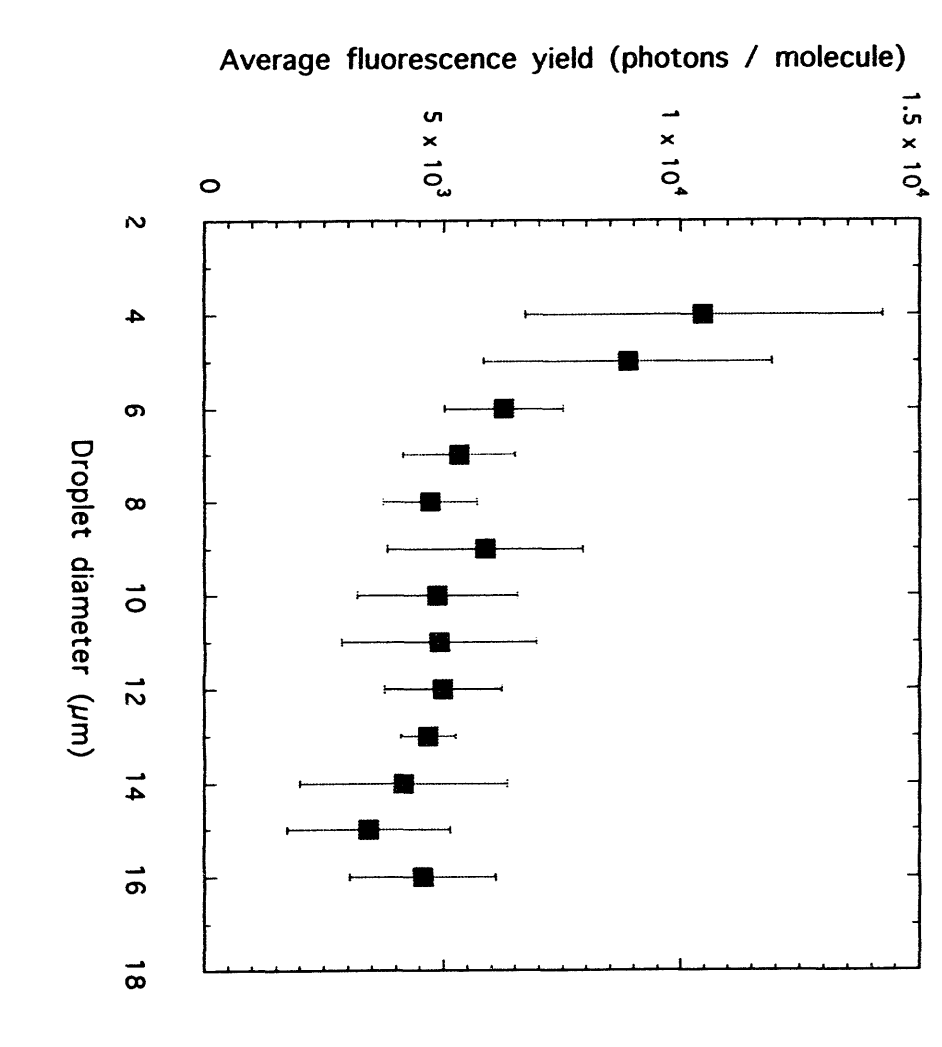


Figure 2. Average fluorescence yield vs. droplet size. Symbols represent an average yield from several droplets of the same size. Error bars are +/- 1 σ .

An estimate of the relative amplitude of cavity-inhibited spontaneous emission can be obtained by relating the observed increase in fluorescence yield for R6G in 4 μm droplets to the emission rate averaged over all molecules in the droplet. As shown by Hirshfeld,³ the integrated fluorescence yield, Φ , is proportional to the ratio A_{sp}/k_{pb} where A_{sp} is the spontaneous emission rate and k_{pb} is the photobleaching rate. Assuming that k_{pb} is unaffected by changes in photon state density (i.e., due only to the local solvent-chromophore environment), we can write an approximate expression for Φ in terms of the inhibited and enhanced emission rate constants, A_i and A_e , and their respective fractions f_i and f_e as

$$\Phi = \Phi_{\text{bulk}}[(A_i/A_h)f_{i+}(A_e/A_h)f_e + f_h]$$
 (2)

where Φ_{bulk} represents the average fluorescence yield in the bulk (droplet diameters > 10 μ m), and A $_b$ and f $_b$ represent the bulk emission rate constant and the respective fraction. The quantity inside the square brackets in Eqn. 2 thus represents the average emission rate (relative to the bulk) over all molecules in the droplet.

If photon emission occurs with roughly equal probability over the free-spectral range (but with different time dependence), it is easily shown that the quantity inside the square brackets in Eq. 2 is equal to 1. That is, the enhancement and inhibition effects exactly cancel and no net increase in the photon yield can occur. The value of Φ for 4 μ m droplets can also be estimated in the other limit where the inhibited fraction, f_i , is equal to zero. The decay constants Ae and Ab are known from our fluorescence lifetime measurements, and the fraction of molecules in the droplet which interact with the droplet MDRs can be estimated from the ratio of modevolume to droplet volume. ^{19,25} For a 4 μ m diameter glycerol droplet, this ratio is approximately 8%, so that $f_e = 0.08$. Substituting a value of 12 for (A_e/A_b) ,6 the fluorescence yield in the limit where $f_i \approx 0$ should be 1.9 times larger than the bulk. The agreement of the measured average fluorescence yield (for R6G in 4 μ m droplets) with the latter limit suggests that the fraction of molecules with an inhibited emission rate is very small. Thus, there must be some mechanism by which the excited state can sample a frequency range large enough to couple emission into the

droplet resonances.

Recently, solvent-chromophore dynamics in liquids have been probed by several different experimental techniques. 12,26,27,28,29 Using time-resolved fluorescence depolarization measurements, Stein and Fayer 12 have shown that the perturbation of the excited state dipole by the solvent results in a dynamical broadening of a spectral line on the same time scall as the radiative lifetime of the chromophore. These authors make the distinction between the fast (fs) thermal motions of the solvent, which give rise to the pure homogeneous dephasing, and the much slower (ns) response of the solvent to the change in the dipole moment of the chromophore upon excitation. The latter process gives rise to spectral diffusion which causes dynamical (time-dependent) broadening of the spectrum. Similar behavior has been also observed in the solid state at cryogenic temperatures by Moerner and co-workers 30 where perturbations due to conformational changes in the host crystal produce center frequency shifts in the fluorescence excitation spectra of single guest molecules.

In the picture described by Stein and Fayer, the spectral linewidth in solution is not fixed, but changes with time. Following an excitation pulse at time near t=0, the linewidth is the homogeneous width that arises from (femtosecond) collisional dephasing due to thermal motion of the solvent molecules. As $t\to\infty$, the chromophore has sampled the entire range of solvent-dipole configurations and the transition can occur at essentially any frequency with some probability give by the inhomogeneous profile. The rate at which the width of a dynamically broadened line changes depends on how fast the solvent molecules can respond to the change in the dipole moment of the chromophore after excitation. From Stein and Fayer's value for the solvent relaxation rate for glycerol at room temperature, the dynamic width is estimated to reach 1/2 of the inhomogeneous width ($\approx 600 \text{ cm}^{-1}$) in a time of roughly 1 fluorescence lifetime (3.6 ns). Thus, the excited state can eventually sample a large enough frequency range to access a cavity resonance irrespective of the initial transition frequency.

These dynamical solvent-chromophore interactions should strongly affect the distribution of emission frequencies and emission times for dye molecules in a liquid microcavity. Consider a transition which has a (nonresonant) center frequency, ω_c , in

the midpoint between two cavity resonance frequencies. At time $t\approx 0$ following excitation, the density of photon states in the range of frequencies within the homogeneous width is small thereby inhibiting emission of a photon. As the spectral line becomes dynamically broadened, there is a significant probability that the emission can occur at a new frequency, ω_c , near a cavity resonance frequency where the photon state density is much higher. This would result in virtually all photon emission to occur near the cavity resonance frequencies provided that the spectral diffusion is sufficiently rapid. Thus, in this scenario, very few photons would be emitted at non-resonant frequencies and thus at an inhibited rate.

In order to illustrate this effect, Monte Carlo calculations were performed to model the distribution of emission times and frequencies in a system where the transition frequency is allowed to randomize on the same time scale as the radiative lifetime. A dynamic width function was approximated³¹ using Stein and Fayer's experimental measurement of the solvent relaxation rate for glycerol at room temperature which defines the spectral width as a function of time. The initial (homogeneous) width was taken to be 100 cm^{-1} fwhm, and the inhomogeneous width at $t = \infty$ was taken to be 600 cm^{-1} fwhm.¹² A "clock" was incremented in 20 picosecond steps, and after each time step a decision was made whether to end the calculation based on a comparison of the integrated emission probability to a random number.

In the Wigner - Weisskopf approximation, 32 the probability of photon emission has a time dependence given by

$$P_{\text{emit}}(\omega,t) = 1 - \exp[-\gamma(\omega) t]$$
 (3)

where we have incorporated a frequency dependence in the decay constant, $\gamma(\omega)$, expressed as

$$\gamma(\omega) = \frac{\rho_{\text{cav}}(\omega)}{\rho_{\text{bulk}}(\omega)} \gamma_0 \tag{4}$$

where $\rho_{cav}(\omega)$ and $\rho_{bulk}(\omega)$ are the cavity and bulk density-of-states functions

respectively, and γ_0 is the decay constant in bulk glycerol (0.27 ns-1).

The approximate photon state density function for the cavity was constructed by assuming a cavity Q of 10^3 and a Lorentzian form for the resonance and a resonance spacing of 700 cm⁻¹; values which should be realistic for a 4 μ m glycerol droplet.³³ We further assumed that, over the frequency range of interest, $\rho_{bulk}(\omega) \approx$ constant. These functions for the cavity and bulk medium were then constrained so that

$$\int_{\Delta_{c}} \rho_{cav}(\omega) d\omega = \int_{\Delta_{c}} \rho_{bulk}(\omega) d\omega$$
 (5)

where Δc is the free spectral range.

In calculating the emission probability, the argument, $\gamma(\omega)$, in Eqn. 3 was taken to be an average over the homogeneous lineshape function, $L(\omega, \omega_c)$, expressed as

$$L(\omega, \omega_c) = \frac{\Gamma}{2 \pi \left[(\omega - \omega_c)^2 + (\Gamma/2)^2 \right]}$$
(6)

where ω_c is the center transition frequency, and Γ is the homogeneous width. The ratio, $\rho_{cav}(\omega_c)/\rho_{bulk}(\omega_c)$ in Eqn. 4 was then replaced by an average value $\langle \rho_{cav}(\omega_c) \rangle/\rho_{bulk}(\omega_c)$ given by

$$\frac{\langle \rho_{cav}(\omega_c) \rangle}{\rho_{bulk}(\omega_c)} = \frac{\int_0^\infty \rho_{cav}(\omega) L(\omega, \omega_c) d\omega}{\int_0^\infty \rho_{bulk}(\omega) L(\omega, \omega_c) d\omega}$$
 (7)

The integrated emission probability was computed at each time step using Eqns. 3 and 7 and compared to a random number generated at the start of the calculation. If the random number is larger, a new center frequency, ω_c , is randomly selected from the time-dependent lineshape function whose width is determined by the dynamic width function using standard Monte Carlo sampling techniques.³⁴ This "diffusion" in frequency space is then continued until the integrated emission probability becomes

greater than the random number and a record is made of the frequency and the time at which the emission occurred.

To illustrate the effect of spectral diffusion in a microcavity environment, two different spectral origins (center frequencies) were chosen. In the first (resonant) case, the origin was chosen to correspond to a cavity resonance, and in the second (non-resonant) case, the origin was located in between two resonances. Figure 3 shows the distribution of emission times for both resonant and non-resonant center frequencies. In both cases, the emission time distribution is described well by single exponential decay with time constants significantly smaller than the bulk decay constant. As expected, the decay constant for the non-resonant case ($\gamma = 0.87$ ns-1) is slightly smaller than for the resonant case ($\gamma = 1.05$ ns-1). Because the transition frequency is not fixed, the result of spectral diffusion in a microcavity is that virtually all emission is coupled out through the resonances.

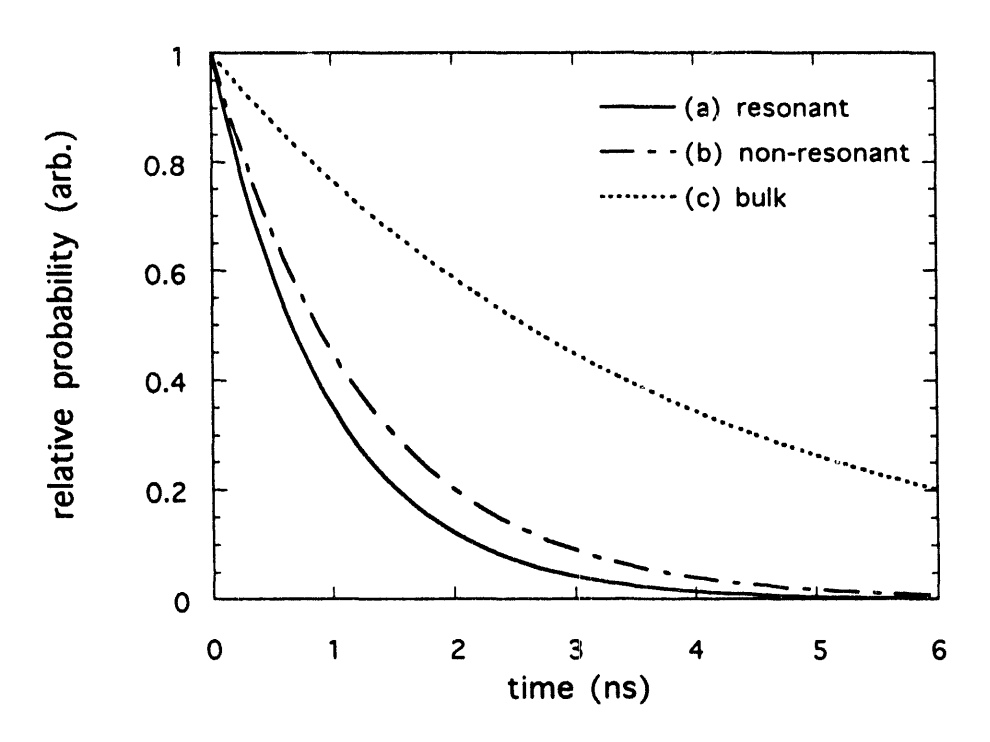


Figure 3. Monte Carlo simulation of emission time distributions for resonant (a), and non-resonant (b) center frequencies. A step size of 20 picoseconds was used with 20000 samples and a homogeneous linewidth of 100 cm⁻¹. Curves are single-exponential fits to the calculated emission time histograms, with decay constants of 1.03 and 0.85 ns⁻¹ for the resonant and non-resonant cases respectively. The dashed curve (c) shows the "bulk" emission time distribution for comparison.

1" 111

This is further illustrated by the simulated distribution of emission frequencies shown in Figure 4. For both resonant and non-resonant cases, the emission frequency distribution maps the cavity resonances with virtually no probability of emission in the 'inhibited' region between the resonances. Similar emission frequency distributions have also been observed experimentally in Fabry-Perot microcavities by Yokoyama and coworkers. Dispersed emission from these structures clearly mapped the cavity resonances and shows very little (if any) emission intensity at non-resonant frequencies

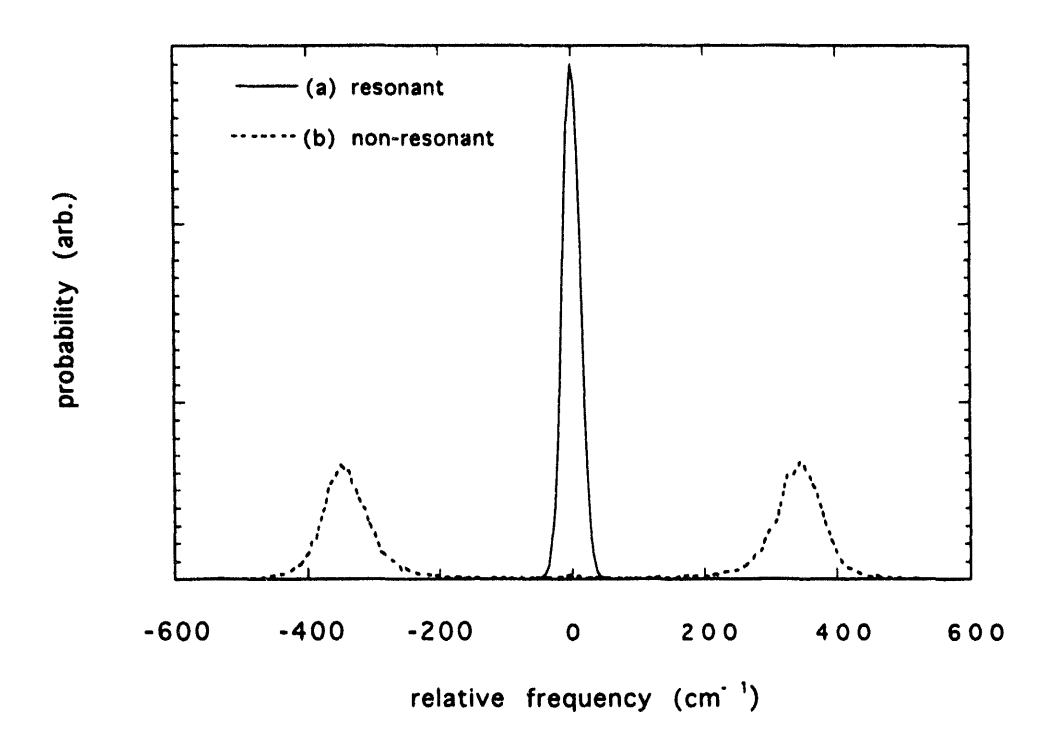


Figure 4. Simulated emission frequency distributions for resonant (a), and non-resonant (b) center frequencies. Both distributions have been normalized to give unit area. The origin of the time-dependent transition frequency distribution was set to zero for both cases. Note that for both (a) and (b), there is negligible probability of photon emission in between the cavity resonances.

The purpose of these calculations was to qualitatively illustrate the effect of solvent-chromophore dynamics on the emission properties of dye molecules in liquid microcavities. We believe that these simulations, in which the transition frequency is

not constrained to be fixed, demonstrate the effect of spectral diffusion in a microcavity environment. Elimination of emission rate inhibition through spectral diffusion is consistent with both the absence of an inhibited component in the previously measured fluorescence decay kinetics and the increased fluorescence yield in the 4 and 5 µm droplets reported here. If one assumes that the fraction of molecules whose emission is inhibited is small compared to the enhanced fraction (an assumption which appears justified on the basis of our model calculations), Eq. 2 predicts that the increase in fluorescence yield should be approximately a factor of 2 which is in good agreement with the experimental results. It therefore seems likely that spectral diffusion strongly influences the distribution of emission frequencies so that emission preferentially occurs near cavity resonances.

If the inhibited emission rate component in our system is truly eliminated through spectral diffusion, it seems important to account for the observation of inhibited emission of chelated europium ions reported by Campillo, et al. In the case of chelated europium species the observed $d \rightarrow f$ transitions involve electrons which are shielded from solvent perturbations. That is, in a case where there is very little inhomogeneous broadening, spectral diffusion cannot occur thus "fixing" the transition frequency. In such a case it seems likely that inhibited emission can occur. In addition, the requirement for elimination of cavity-inhibited emission through spectral diffusion is that the solvent reorganization occur on the same time scale as the excited state lifetime. If the solvent response time is much longer than the free-space radiative lifetime (i.e., in a glass or solid matrix), it then seems likely that, in such a case, the distribution of emission times will show an inhibited component.

Summary and Conclusions

Measurements of R6G fluorescence yields in microdroplets have revealed a size dependence which is attributed to a net decrease in the probability per absorption-emission cycle of photochemical bleaching. This effect derives from an increase in the average spontaneous emission rate as a result of coupling of emission into droplet MDRs. A two-fold increase in the average number of fluorescence photons detected per molecule has been observed for R6G in 4 μ m droplets over the yield measured at larger diameters which is interpreted in terms of a net increase in the average spontaneous emission rate. These results are consistent with previously

measured R6G fluorescence decay kinetics in microdroplets and suggest that the relative amplitude of cavity-inhibited emission in this system is very small. We have proposed a mechanism based on randomization of transition frequencies on a time-scale comparable to the excited state lifetime, illustrated by simple Monte Carlo calculations, which can account for the virtual elimination of cavity-inhibited emission in this system. It is also clear from these results that cavity-QED effects associated with microdroplets offer a substantial sensitivity advantage for fluorescence detection of single molecules.

Acknowledgements

This research was sponsored by the U.S. Department of Energy, Office of Basic Energy Sciences, under contract DE-AC05-84OR21400 with Martin Marietta Energy Systems. MDB acknowledges an appointment to the ORNL postdoctoral research associate program administered by the Oak Ridge Institute for Science and Education and Oak Ridge National Laboratory. The authors would also like to thank Steven C. Hill for many helpful discussions.

References

- ¹ W. B. Whitten, J. M. Ramsey, B. V. Bronk, and S. Arnold, Anal. Chem. **63**, 1027 (1991); K. C. Ng, W. B. Whitten, J. M. Ramsey, and S. Arnold, *ibid*. 64, 2914 (1992); M. D. Barnes, K. C. Ng, W. B. Whitten, and J. M. Ramsey, *ibid*. 65, 2360 (1993).
- ² P. Pringsheim, Fluorescence and Phosphorescence (Interscience, New York, 1949).
- ³ T. Hirschfeld, Appl. Opt. **15**, 3135 (1976).
- ⁴ E. M. Purcell, Phys. Rev. **69**, 681 (1946).
- ⁵ S. Haroche, and D. Kleppner, Phys. Today **42** (1), 24 (1989); S. E. Morin, Q. Wu, and T. W. Mossberg, Opt. Photonics News **3**, 8 (1992), and references cited therein.
- ⁶ M. D. Barnes, W. B. Whitten, S. Arnold, and J. M. Ramsey, J. Chem. Phys. 97, 7842 (1992).
- ⁷ H-B. Lin, J. D. Eversole, C. D. Merrit, and A. J. Campillo, Phys. Rev. A 45, 6756 (1992).
- ⁸ D. Kleppner, Phys. Rev. Lett. **47**, 233 (1981); R. G. Hulet, E. S. Hilfer, and D. Kleppner, *ibid* **59**, 2955 (1987).
- 9. F. DeMartini, G. Innocenti, G. R. Jacobvitz, and P. Mataloni, Phys. Rev. Lett. 59, 2955 (1987).
- ¹⁰W. Jhe, A. Anderson, E. A. Hinds, D. Meschede, L. Moi, and S. Haroche, Phys. Rev. Lett. 58, 666 (1987).
- ¹¹ D. J. Heinzen, J. J. Childs, J. E. Thomas, and M. S. Feld, Phys. Rev. Lett. **58**, 1320 (1987).
- ¹² A. D. Stein, and M. D. Fayer, J. Chem. Phys. **97**, 2948 (1992).
- ¹³ R. Kubo, Adv. Chem. Phys. **15**, 101 (1969).
- ¹⁴ E. Fermi, Rev. Mod. Phys. 4, 87 (1932).

- ¹⁵ S. C. Ching, H. M. Lai, and K. Young, J. Opt. Soc. Am. B. 4, 1995 (1987).
- ¹⁶ H. Yokoyama, and S. D. Brorson, J. Appl. Phys. **66**, 4801 (1989).
- ¹⁷ See S. C. Hill, and R. E. Benner, in *Optical Effects Associated With Small Particles*, edited by P. W. Barber and R. K. Chang (World Scientific, Singapore, 1988).
- ¹⁸ A. J. Campillo, J. D. Eversole, and H-B. Lin, Phys. Rev. Lett. **67**, 437 (1991).
- ¹⁹ H-M. Tzeng, K. F. Wall, M. B. Long, and R. K. Chang, Opt. Lett. **9**, 499 (1984).
- ²⁰ H-B. Lin, J. D. Eversole, and A. J. Campillo, J. Opt. Soc. Am. B 9, 43 (1992).
- ²¹ L. M. Folan, S. Arnold, and S. Druger, Chem. Phys. Lett. 118, 322 (1985); S. Arnold, and L. M. Folan, Optics Lett. 14, 387 (1989).
- ²² R. F. Weurker, H. Shelton, and R. V. Langmuir, J. Appl. Phys. 30, 342 (1959).
- ²³ S. Arnold, and L. M. Folan, Rev. Sci. Instrum. 57, 2250 (1986).
- ²⁴ A. Ashkin, and J. M. Dziedzic, Appl. Opt. 20, 1803 (1981).
- ²⁵ P. T. Leung, and K. Young, J. Chem. Phys. **89**, 2894 (1988)
- ²⁶ C. J. Bardeen, and C. V. Shank, Chem. Phys. Lett. **203**, 535 (1993).
- ²⁷ B. Sauter, and C. Bräuchle, Chem. Phys. Lett. **204**, 157 (1993).
- ²⁸ M. J. E. Morgenthaler, S. R. Meech, and K. Yoshihara, Chem. Phys. Lett. **197**, 537 (1992).
- ²⁹ E. T. J. Nibbering, D. A. Wiersma, and K. Duppen, Phys. Rev. Lett. 66, 2464 (1991).
- ³⁰ W. P Ambrose, Th. Basche', and W. E. Moerner, J. Luminescence **53**, 62 (1992); Th. Basche', W. P Ambrose, and W. E. Moerner, J. Opt. Soc. Am. B **9**, 829 (1992); W. P. Ambrose, and W. E.

- . Moerner, Nature (London) 349, 225 (1991).
 - ³¹ From inspection of Fig. 1 in Ref. 8, the approximate functional form for the dynamic width function $d(\Delta w)/dt$ corresponding to a solvent relaxation rate, R=0.5, was chosen to be $0.5(t/\tau_r)^{-0.4}$, where τ_r is the free-space radiative lifetime.
 - ³² V. Weisskopf, and E. P. Wigner, Z. Phys. **63**, 54 (1930).
 - ³³ P. Chylek, J. Opt. Soc. Am. 66, 285 (1976).
 - ³⁴ M. Karplus, R. N. Porter, and R. D. Sharma, J. Chem. Phys. 43, 3259 (1965).
 - ³⁵ H. Yokoyama, M. Suzuki, and Y. Nambu, Appl. Phys. Lett. **58**, 2598 (1991).

DISCLAIMER

This report was prepared as an account of work sponsored by an agency of the United States Government. Neither the United States Government nor any agency thereof, nor any of their employees, makes any warranty, express or implied, or assumes any legal liability or responsibility for the accuracy, completeness, or usefulness of any information, apparatus, product, or process disclosed, or represents that its use would not infringe privately owned rights. Reference herein to any specific commercial product, process, or service by trade name, trademark, manufacturer, or otherwise does not necessarily constitute or imply its endorsement, recommendation, or favoring by the United States Government or any agency thereof. The views and opinions of authors expressed herein do not necessarily state or reflect those of the United States Government or any agency thereof.

DATE FILMED 10/17/94

